AGU PUBLICATIONS

JGR

Journal of Geophysical Research: Atmospheres

RESEARCH ARTICLE
10.1002/2013JD020688

Key Points:
- Influence of boreal summer blocking on circulation in East Asia was examined
- Okhotsk blocking is systematically affecting the area as the most dominant mode
- The blocking showed +/- correlations with precipitation/temperature in summer

Correspondence to:
J.-B. Ahn,
jbahn@pusan.ac.kr

Citation:
Park, Y.-J., and J.-B. Ahn (2014), Characteristics of atmospheric circulation over East Asia associated with summer blocking, *J. Geophys. Res. Atmos.*, *119*, doi:10.1002/2013JD020688.

Received 9 AUG 2013
Accepted 31 DEC 2013
Accepted article online 5 JAN 2014

Characteristics of atmospheric circulation over East Asia associated with summer blocking

Yong-Jun Park[1] and Joong-Bae Ahn[1]

[1]Division of Earth Environmental System, Pusan National University, Busan, Republic of Korea

Abstract The boreal summer-blocking regions were defined using the reanalysis data over the three decades of 1981–2010, and the influence of the blocking on atmospheric circulation in East Asia was examined. The summer blocking occurred mostly in North Europe, Ural region, Sea of Okhotsk (OK), and northeastern Pacific. The summer blocking was the major mode in these four regions according to principal component analysis using 500 hPa geopotential heights. Among the four blocking regions, OK blocking frequencies (OK BFs) showed negative and positive correlations with summer temperature and precipitation of Northeast Asia centered around the East Sea/Sea of Japan, respectively. In particular, the OK BF had a statistically significant correlation coefficient of −0.54 with summer temperatures in the Korean Peninsula. This indicates that the summer temperature and precipitation in this region were closely related to the OK blocking. According to the composite analysis for the years of higher-than-average BF (positive BF years), the OK High became stronger and expanded, while the North Pacific High was weakened over the Korean Peninsula and Japan and an anomalously deep trough was developed in the upper layer (200 hPa). As the cool OK High expanded, the temperature decreased over Northeast Asia centered around the East Sea/Sea of Japan and the lower level (850 hPa) air converged cyclonically, resulting in the increased precipitation, which induced the divergence in the upper layer and thereby strengthened the jet stream. Thus, the boreal summer OK blocking systematically influencing the area as the most dominant mode.

1. Introduction

In the summer of 2010, a strong Euro-Russian blocking caused an intense heat wave in eastern Europe and western Russia. The maximum temperatures exceeded 40°C in the region, resulting in significant damage to industry and the economy and numerous fatalities [*Matsueda*, 2011]. *Tyrlis and Hoskins* [2008] noted that blocking at 500 hPa is one of the reasons causing anomalous synoptic-scale atmospheric change. The pressure ridge that persists for a long time at the upper level of the middle latitudes, defined as a blocking, prevents westerly winds and hinders the progression of cyclones moving eastward [*Berggren et al.*, 1949].

Over the past several decades, several different blocking indices had been developed. *Rex* [1950] developed an empirical and quantitative definition of the blocking index from 500 hPa geopotential gradient, which became the most commonly used blocking index in other studies [e.g., *Lejenäs and Øakland*, 1983; *Tibaldi and Molteni*, 1990; *Lupo and Smith*, 1995; *Trigo et al.*, 2004; *Barriopedro et al.*, 2006]. *Pelly and Hoskins* [2003] defined the blocking using a potential vorticity-potential temperature index. *Diao et al.* [2006] developed a two-dimensional blocking index that is similar to the index suggested by *Tibaldi and Molteni* [1990].

Renwick and Wallace [1996] insisted that blocking activity in Northern Hemisphere Pacific increased (decreased) during winter in the La Niña (El Niño) years. In contrast, *Renwick* [1998], *Marques and Rao* [2000], and *Wiedenmann et al.* [2002] showed that the Southern Hemisphere revealed more frequent blocking during the El Niño years than during the La Niña years. *Shabbar et al.* [2001] suggested that the frequency of blocking in the Northern Hemisphere increased during the negative North Atlantic Oscillation (NAO) years compared to that in the positive NAO years during the winter. However, the impacts of the El Niño–Southern Oscillation (ENSO) and Arctic Oscillation (AO) on blocking have not yet been clearly revealed. The relationships of the blocking with the ENSO and AO vary seasonally and regionally.

The East Asian monsoon system is one of the most energetic components of the global climate system [*Wang et al.*, 2001], and East Asia surrounding the Korean Peninsula is a representative region with a strong characteristic of a prevailing seasonal monsoon [*Jang and Jhun*, 2004]. *Lee and Jhun* [2006] claimed that the winter monsoon intensity

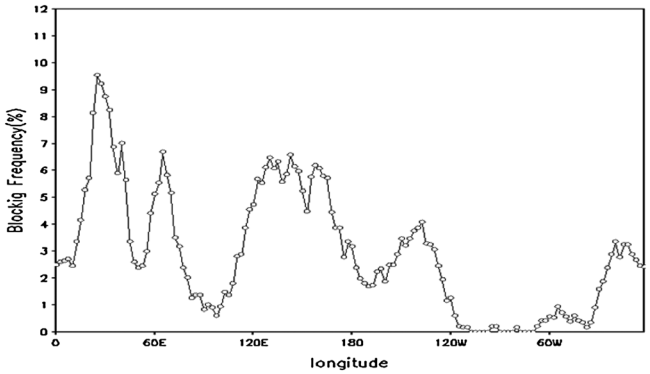

Figure 1. Average blocking frequency (BF) of the boreal summer for the period of 1981–2010.

in East Asia is influenced by the occurrence and duration of stagnant pressure pattern which causes anomalous warm or cold waves. In addition, *Lee and Jhun* [2007] postulated a strong negative relationship between winter temperature and blocking over the Korean Peninsula. *You and Ahn* [2012] determined that the blocking mode of winter in the North Pacific to be the second major mode after the AO using empirical orthogonal function (EOF) analysis and analyzed its influence in terms of atmospheric and oceanic variables. However, most of the studies examining the regional influences of blocking on climate and weather variations have focused on winter.

Summer blocking is generally weaker than winter blocking [*Wiedenmann et al*., 2002]. However, *Wang* [1992] examined blocking high activity during the Northeast Asian summer monsoon (known as *Meiyu* in China, *Changma* in Korea, and *Bai-u* in Japan) and found that the blocking highs over the Okhotsk Sea had an obvious effect on the *Meiyu* in the Yangtze River and Huaihe River Basin. *Wang and Lupo* [2009] showed that southeastward wave flux from the upstream area of the Sea of Okhotsk over much of the North Pacific in the midlatitudes is associated with a strong preceding El Niño event, the development of the Okhotsk High, and a negative 500 hPa geopotential height/sea surface temperature (SST) anomaly around the coherent region. *Rimbu and Lohmann* [2011] attributed the blocking activity in the Euro Atlantic during summer to the unusual temperatures over southwest Greenland. *Kung et al*. [1992] simulated the control experiment to understand the summer-blocking pattern. However, little research has been conducted on the summer blocking over East Asian regions despite the need for a proper understanding of the phenomena due to its impact on weather and climate.

This paper, therefore, investigates the correlation between the blocking and the summer climate in East Asia. Descriptions about used data and how to select blocking index are expressed in section 2, and the analyzed characteristics of summer blocking are presented in section 3. The relationships between a climate index and blocking and the characteristics of East Asian climate are examined in section 4. Lastly, the paper concludes with a discussion in section 5.

2. Data Sets and Methods

2.1. Data

The data set used in this study was the National Centers for Environmental Prediction/National Center for Atmospheric Research Reanalysis 1 data with 2.5° × 2.5° gridded daily geopotential height and monthly sea

Table 1. BFs at Each Sector Defined in the Study (Unit: %)

	Blocking Region			
Sector	NE BF	UR BF	OK BF	NP BF
Domain	0°E–50°E	50°E–80°E	120°E–160°E	160°E–130°W
Mean_BF	5.21% (30 years)	3.99% (30 years)	5.82% (30 years)	3.18% (30 years)
PBFY_BF	8.35% (15 years)	7.24% (14 years)	9.69% (14 years)	7.02% (11 years)
NBFY_BF	2.06% (15 years)	1.14% (16 years)	2.44% (16 years)	0.96% (19 years)

Table 2. Correlation Coefficients Between the Regional BF and the EOF Principal Component (PC) Time Series of 500 hPa Geopotential Anomaly Height for JJA[a]

	NE BF 0°E–50°E	UR BF 50°E–80°E	OK BF 120°E–160°E	NP BF 160°E–130°W
EOF mode PC1	0.61**	0.68**	0.51**	0.58**
EOF mode PC2	−0.12	−0.15	0.34	0.31

[a]Level of significance: **, significant at 1% level.

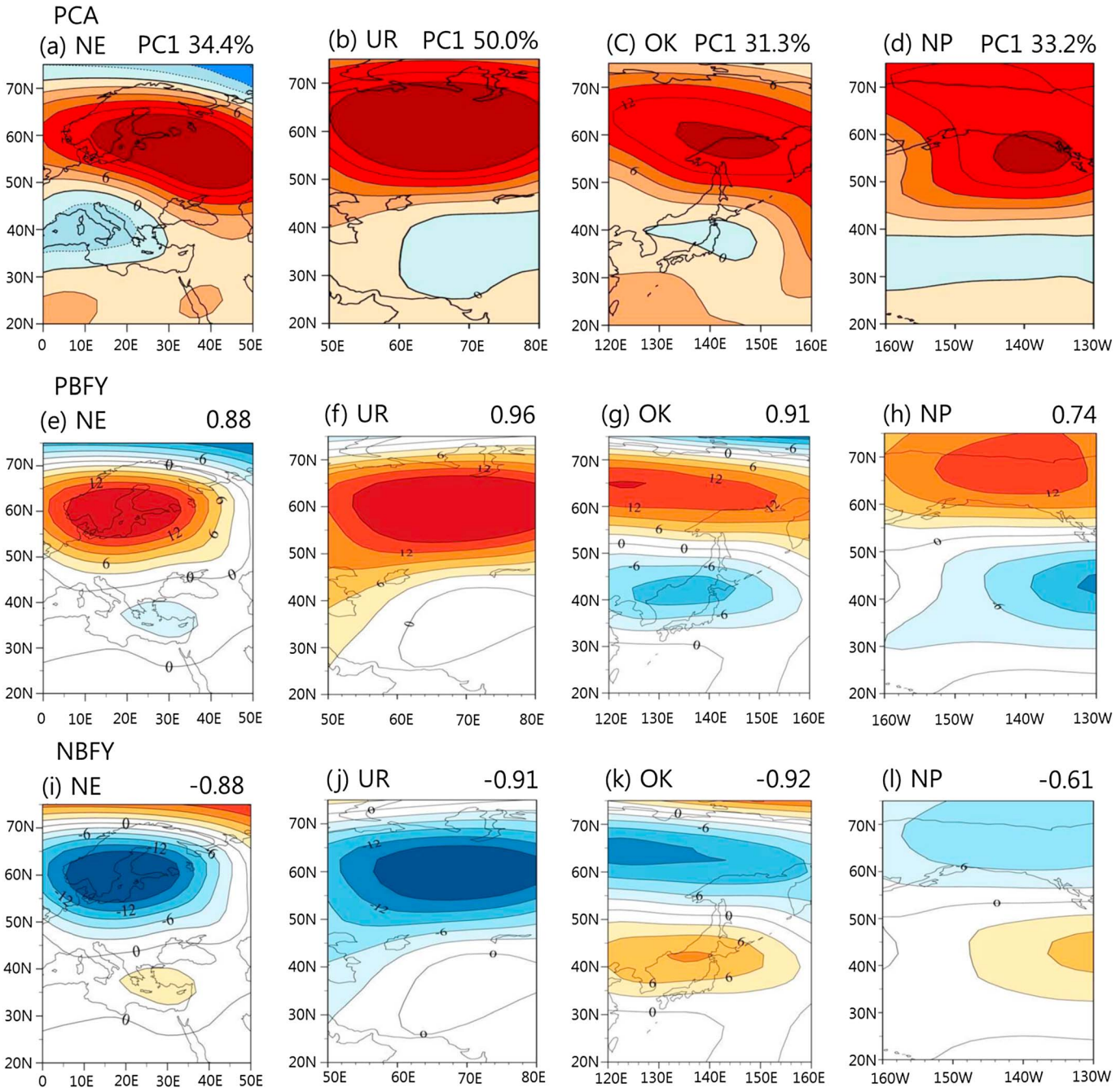

Figure 2. (a–d) PCA mode EOF1 and composite anomaly for (e–h) PBFY and (i–l) NBFY summers. The numbers in upper right corner of Figures 2a–2d are the percentage of the EOF1 mode, and the number in Figures 2e–2l are the spatial correlation coefficients between the EOF1 mode and PBFY/NBFY.

Table 3. Variation of Four Regional BFs in Positive and Negative AO Years[a]

	Blocking Region				
	NE BF	UR BF	OK BF	NP BF	Total BF
Positive AO year	5.75	4.83	5.42	5.18	3.28
Negative AO year	4.12	1.35	6.16	6.32	2.94

[a]Total BF is average over all longitudes (unit: %).

level pressure (SLP), air temperature, wind, and vertical velocity for the period 1981–2010. Precipitation data provided by the Global Precipitation Climatology Project of the National Oceanic and Atmospheric Administration and Extended Reconstructed Sea Surface Temperature data for the period 1981–2010 with 2°×2° grid were used. The temperature and precipitation observed at 62 in situ stations in South Korea for the same period were also utilized.

2.2. Definition of the Blocking Index

The blocking index developed by *Tibaldi and Molteni* [1990], further used by *Barriopedro et al*. [2006] and *You and Ahn* [2012], is utilized in this study. The blocking index was calculated using daily 500 hPa geopotential height gradients of summer for 30 years (1981–2010).

The 500 hPa geopotential height gradients (GHG) at north and south (GHGN and GHGS, respectively) of latitude ($\phi 0$) have been computed at each 2.5° longitude intervals as follows:

$$\begin{aligned} \mathrm{GHGN}(\lambda) &= \frac{Z(\lambda,\phi_N) - Z(\lambda,\phi_0)}{\phi_N - \phi_0}, \\ \mathrm{GHGS}(\lambda) &= \frac{Z(\lambda,\phi_0) - Z(\lambda,\phi_S)}{\phi_0 - \phi_S}, \end{aligned} \tag{1}$$

where $Z(\lambda,\phi)$ is the 500 hPa height geopotential at longitude (λ) and latitude (ϕ). Here $\phi_N = 77.5°\mathrm{N} + \Delta$, $\phi_0 = 60.0°\mathrm{N} + \Delta$, $\phi_S = 40.0°\mathrm{N} + \Delta$, and $\Delta = -5.0°, -2.5°, 0.0°, 2.5°, 5.0°$. Five GHGN($\lambda$)s and GHGS($\lambda$)s were computed at each latitude, λ. A blocking was considered to have occurred at a latitude, λ, when GHGN(λ) is less than −10 geopotential meters (gpm) per latitude with a GHGS(λ) larger than 0 at least one value of among the five Δs.

In addition, a minimum of five consecutive blocked days were defined as one blocking event. The blocking frequency (BF) was represented as the percentage rate of blocking days during the boreal summer (June–August, JJA).

Figure 1 shows average BF for JJA along the latitude. The summer blocking was the most frequent over Europe (30°E), and the second peak appeared over Okhotsk (120°E–160°E). The four major blocking regions examined were North Europe (NE), Ural region (UR), Sea of Okhotsk (OK), and northeastern Pacific (NP), as shown in Table 1.

The years of higher-than-average BF and lower-than-average BF were defined as positive BF year (PBFY) and negative BF year (NBFY), respectively, for convenience.

3. Characterization of Summer Blocking

Principal component analysis (PCA) was conducted using 500 hPa geopotential anomaly after removing the trend for the four major blocking areas. Table 2 shows the temporal correlation coefficients between BFs and

Table 4. Same as in Table 3 but for El Niño, La Niña, and Neutral Years[a]

	Blocking Region				
	NE BF	UR BF	OK BF	NP BF	Total BF
El Niño year	6.04	2.70	6.54	4.79	3.22
La Niña year	5.73	4.38	3.08	3.27	2.23
Neutral year	4.67	4.38	6.50	2.48	3.06

[a]Total BF is average over all longitudes (unit: %).

Table 5. Summer BFs (%) During the Positive/Negative AO and El Niño/La Niña Years[a]

	Positive AO				Negative AO				Nonpositive/Nonnegative AO			
	NE	UR	OK	NP	NE	UR	OK	NP	NE	UR	OK	NP
El Niño year	−(0)	−(0)	−(0)	−(0)	5.15(4)	1.69(4)	5.39(4)	7.21(4)	7.23(3)	4.04(3)	8.08(3)	1.56(3)
La Niña year	−(0)	−(0)	−(0)	−(0)	−(0)	−(0)	−(0)	−(0)	5.73(6)	4.38(6)	3.08(6)	3.27(6)
Neutral year	5.75(4)	4.83(4)	5.42(4)	5.18(4)	0.00(1)	0.00(1)	9.27(1)	2.76(1)	4.71(12)	4.56(12)	6.62(12)	1.56(12)

[a]Figures in parentheses refer to the numbers of occurrence year.

EOF of the first and second modes for each region. In the first modes of EOF, the correlations coefficients between 500 hPa geopotential height and NE, UR, OK, and NP averaged BFs were 0.61, 0.68, 0.51, and 0.58, respectively. They were all higher than the 1% significance level, implying that the first mode of EOF is highly correlated with the blocking at each region. However, the BFs were only weakly correlated with the rest of the EOF modes for each region.

In Figure 2, the spatial patterns of the first mode of EOF for each region, which are closely related with the boreal summer blockings, are compared with the composited PBFY and NBFY fields. The spatial patterns of the first mode of EOF for each region were quite close to the corresponding PBFY fields. The spatial correlation coefficients between the first mode of EOF and the PBFY field for each region were all higher than the 1% significance level. Moreover, the spatial patterns of NBFY for each region were almost identical and opposite in sign with respect to PBFY, indicating that the blocking in each region was the most dominant phenomenon and appears systematically during the boreal summer.

4. Summer Blocking and the East Asia Climate

4.1. Regional Summer Blocking and Climate Indices: The AO and ENSO

To determine the relationships between summer blocking at the four different regions and the AO, years of the positive and negative AO were defined as the year of the AO index higher (1983, 1989, 1994, and 1996) and lower (1987, 1993, 1997, 2004, and 2009) than 1 standard deviation, respectively. The AO index provided by the Climate Prediction Center (CPC) for the period 1981–2010 was used in this study. Table 3 shows the BFs of the four regions during the positive and negative AO years. The NE and UR BFs were higher during the positive AO years than during the negative years. On the contrary, in the negative AO years, the OK and NP BFs were higher than in the positive years. That is, the summer BF tended to increase during the negative AO years in OK and NP but increased during the positive AO years in NE and UR. *Shabbar et al.* [2001] showed that the winter BF in the northern hemisphere Atlantic increased during the negative NAO compared to the positive period. Our results indicate that the summer and winter NE BFs might be related oppositely with the AO.

The BFs of the four different regions were also classified into three categories using the Niño 3.4 index provided also by the CPC for the period 1981–2010: the El Niño, the La Niña years, and Neutral years (Table 4). The El Niño (1982, 1987, 1991, 1997, 2002, 2004, and 2009) and La Niña years (1985, 1988, 1998, 1999, 2000, and 2010) were classified as the year of higher and lower than 1 standard deviation, respectively. In summer, the NE and NP BFs were increased during the El Niño years, while UR and OK BFs were decreased during the El Niño and La Niña years, respectively.

Renwick and Wallace [1996], *Wiedenmann et al.* [2002], and *Barriopedro et al.* [2006] showed that Northern Hemispheric winter blocking increases during the La Niña years. This result indicates that OK BF decreases in La Niña years of summer, in contrast to winter.

Table 5 shows the summer BFs during the positive/negative AO and El Niño/La Niña years. The BFs of the nonpositive/nonnegative AO year were always larger than those of the positive and negative AO years in the NE, UR, and OK regions except NP region in the El Niño and La Niña years. The BFs during the Neutral year decreased (increased) in the NE, UR, and NP regions and increased (decreased) in the OK region during the negative and nonpositive/negative (positive) AO years compared to the mean BFs in Table 1. Further studies are needed to understand physical relationships between the AO, El Niño, and blocking in summer.

Table 6. Correlation Coefficients Between Regional BFs and Temperature and Precipitation in the Korean Peninsula for JJA[a]

	Temperature	Precipitation
NE BF	0.02	−0.34
UR BF	0.05	0.23
OK BF	−0.54**	0.15
NP BF	0.18	0.01

[a]Level of significance: **, significant at 1% level.

4.2. Correlations With Temperature and Precipitation Over Northeast Asia and the Korean Peninsula

In this section, the relationships between blockings occurred in the four regions and summer temperature and precipitation of the Northeast Asia including the Korean Peninsula are analyzed. According to Table 6, the temporal correlation coefficient between OK BF and the summer average temperature of the Korean Peninsula was −0.54 (significant at the 1% level). However, NE, UR, and NP BFs showed statistically insignificant relationships with the temperature. This result indicates that the summer temperature of the Korean Peninsula is mainly dependent on the change of OK blocking. However, the correlation coefficients between all BFs and precipitation were not statistically significant. Considering the fact that summer precipitation and temperature are negatively correlated in South Korea [*Ahn et al.*, 1997], the present result is different because OK BF is highly correlated with temperature but poorly correlated with precipitation in this analysis. This can be attributed to the local characteristics of the precipitation during summer in this region. This result is discussed in more detail in the next section.

Figure 3 shows the correlation of OK BF and monthly temperature and precipitation in East Asia (110°E–150°E, 20°N–70°N). The correlation between OK BF and summer temperature showed a tripole pattern in East Asia, with a positive correlation around 65°N and 25°N and a negative correlation around 40°N. The negative correlation in the Korean Peninsula and Japan centered around the Sea of Japan (East Sea, hereafter) was statistically significant at the 5% level. OK BF and summer precipitation (Figure 3b) showed a negative correlation around 65°N and 25°N, and a positive correlation around 40°N of Japan and the East Sea. Thus, the correlation pattern of temperature and precipitation of East Asia showed a similar structure with a reversed sign, implying close relationships between the variables and OK BF. Although the correlation coefficient between OK BF and summer precipitation over the Korean Peninsula was relatively low, as can be seen from the figure, in terms of synoptic scale, the tripole structures of temperature and precipitation indicate that they are closely correlated and systematically influenced by blocking in East Asia. The low temperature and the high precipitation over the northeast Asia in Figure 3 are closely related to the anomalous low pressure system shown in Figures 2g–2i.

Overall, the results suggest that the summer precipitation is negatively related with the temperature in East Asia in association with OK blocking.

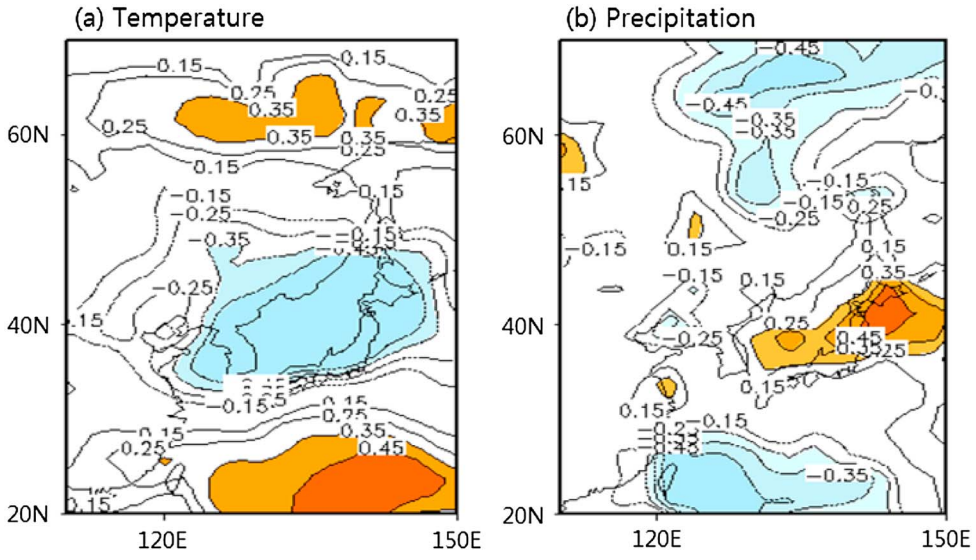

Figure 3. Correlation coefficients between OK BF and normalized mean temperature and precipitation in East Asia for JJA. Shaded areas indicate the 5% significance level.

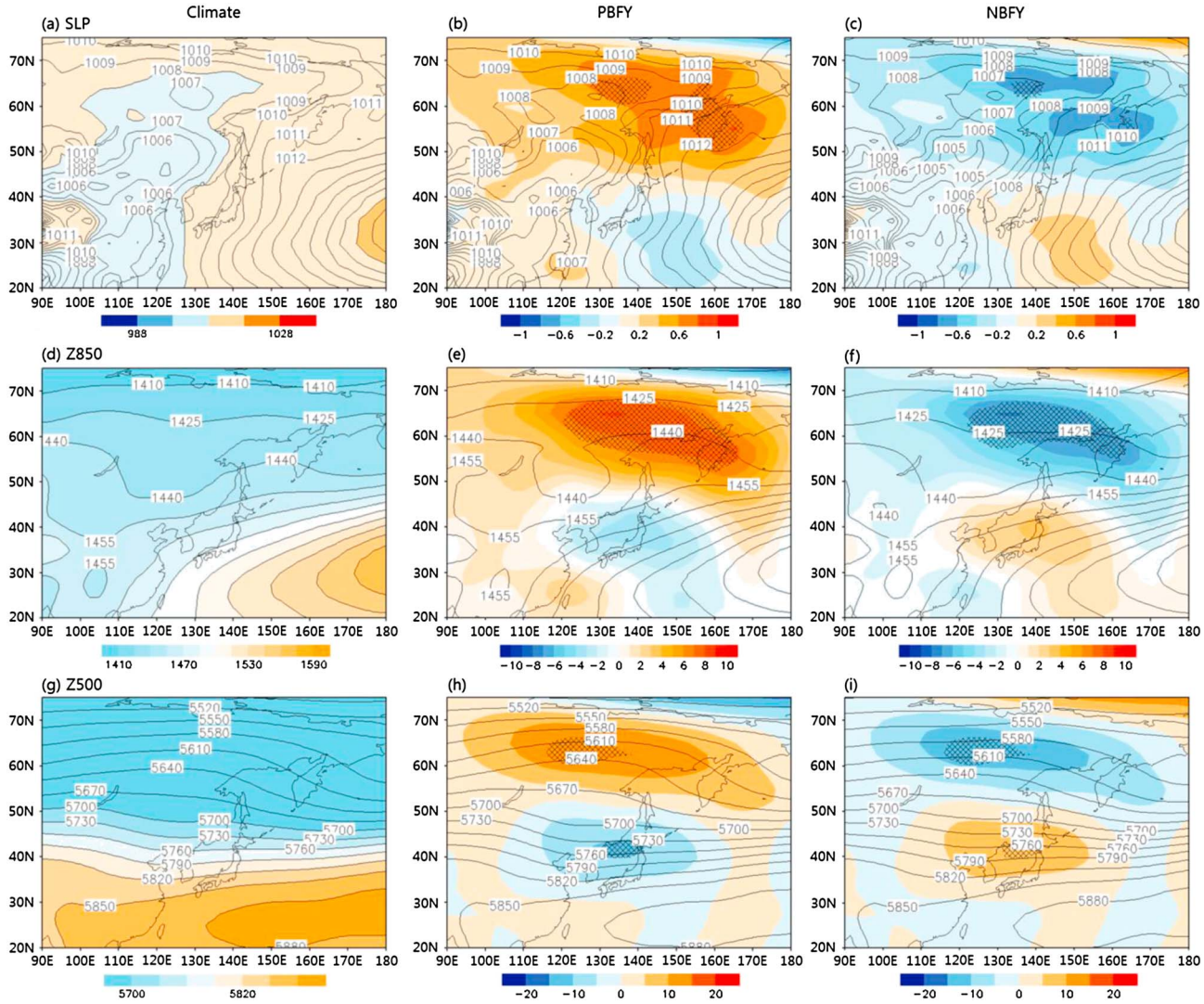

Figure 4. (a–c) Mean fields of SLP, and geopotential height at (d–f) 850hPa and (g–i) 500hPa for climate mean (Figures 4a, 4d, and 4g), PBFY composite (Figures 4b, 4e, and 4h), and NBFY composite (Figures 4c, 4f, and 4i). Contours for PBFY and NBFY indicate the mean over these events, whereas shaded regions show their anomaly compared to the climate mean (unit: gpm). The reticula indicate the regions of 10% significance level.

4.3. Characteristic of Atmospheric Circulation Over East Asia Including the Korean Peninsula

To investigate the change of atmospheric circulation over East Asia associated with the OK blocking, anomalous PBFY and NBFY anomaly composite fields of surface, 850 hPa, and 500 hPa geopotential height are shown, along with their climatology, in Figure 4. Climatologically, East Asia is dominantly influenced by the North Pacific High during summer. In the years of positive blocking, positive and negative anomalous fields formed dipole-like pattern in the meridional direction slightly shifted to the west [*Wang and Lupo*, 2009]. This indicates the strengthened OK High reinforced by positive SLP anomaly around the Sea of Okhotsk, Kamchatka Peninsula, and mountainous region of the Sakha Republic of Russia, and weakening of pressure around the edge of Northwest Pacific High during PBFY. As a result, the SLP deepens around the East Sea, particularly over the Korean Peninsula and Japan. During NBFY, in contrast, OK High is weakened by negative SLP anomaly at Sea of Okhotsk and positive SLP anomaly is located around the East Sea, which strengthens the North Pacific High in the region and induces more zonal geopotential distribution at the upper layers. The spatial structures of geopotential height anomaly composite are similar to the first EOF mode shown in Figure 2. This means that the dipole structure is the major pattern associated with summer blocking in this area. In addition, the blocking appears systematically in this region since the distributions of PBFY and NBFY are similar and have the opposite sign.

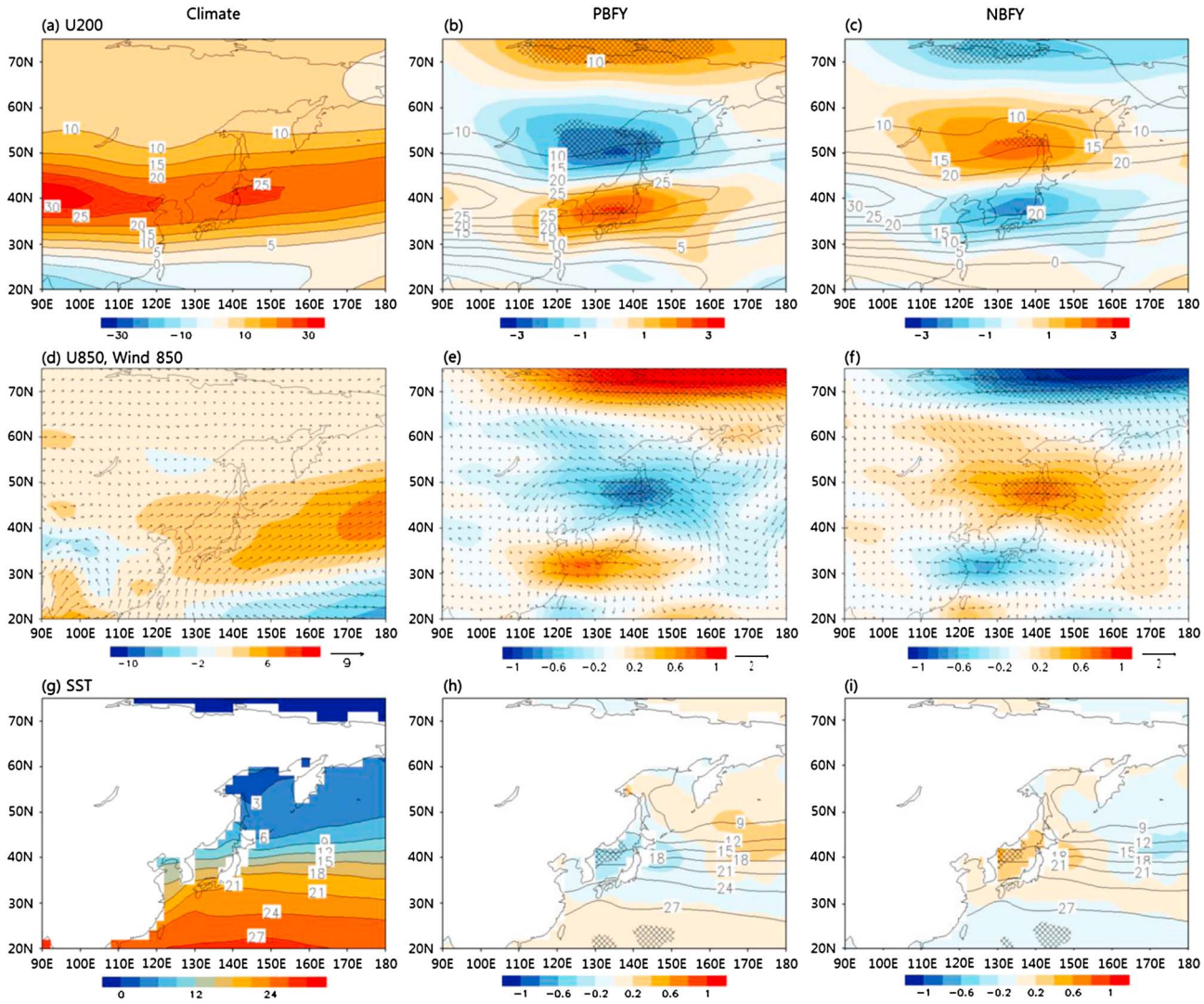

Figure 5. Same as in Figure 4 but for the zonal wind (m/s) at (a–c) 200hPa and (d–f) 850hPa and (g–i) SST (°C). The reticula indicate the regions of 10% significance level.

Figure 5 shows the PBFY and NBFY composite fields for the 200 hPa zonal wind (Figures 5a, 5d, and 5g), 850 hPa wind vector (arrow) and speed (shaded) (Figures 5b, 5e, and 5h), and SST (Figures 5c, 5f, and 5i). The strong upper layer jet is generally located along the belt of 40°N latitude (Figure 5a). Warm air is transferred from the South China Sea along the edge of North Pacific High by 850 hPa wind toward the Northwest Pacific, including the Japanese islands and the Korean Peninsula by the southwesterly (Figure 5b). As shown in Figure 4, decreased GHG around 40–60°N during PBFY induces a weakening of 200 hPa zonal wind around 50°N area. While the jet stream at 200 hPa located around 35–40°N has further strengthened due to the reinforced anomalous westerly winds induced by increased GHG (Figure 5d). In the 850 hPa wind field, positive and negative anomalies are formed, respectively, in southwestern Japan (30°N) and Sakhalin (50°N), thereby creating anomalous cyclonic circulation centered on the East Sea. On the contrary, during NBFY, westerly wind in 200 hPa becomes stronger around 50°N where GHG is increased, but weaker around 35–40°N. Negative and positive 850 hPa geopotential anomalies are formed in southwestern Japan (30°N) and Sakhalin (50°N), respectively, thereby inducing anomalous anticyclonic circulation centered on the East Sea. According to the change in the pressure field, wind circulations during PBFY and NBFY showed opposite patterns. Systematic changes of SST in conjunction with OK BF also appeared. During PBFY, a positive anomaly is located at the center of the North Pacific and a negative anomaly at the northeast marginal seas such as the East Sea, the northeast of Japan, and Yellow sea, and vice versa during NBFY.

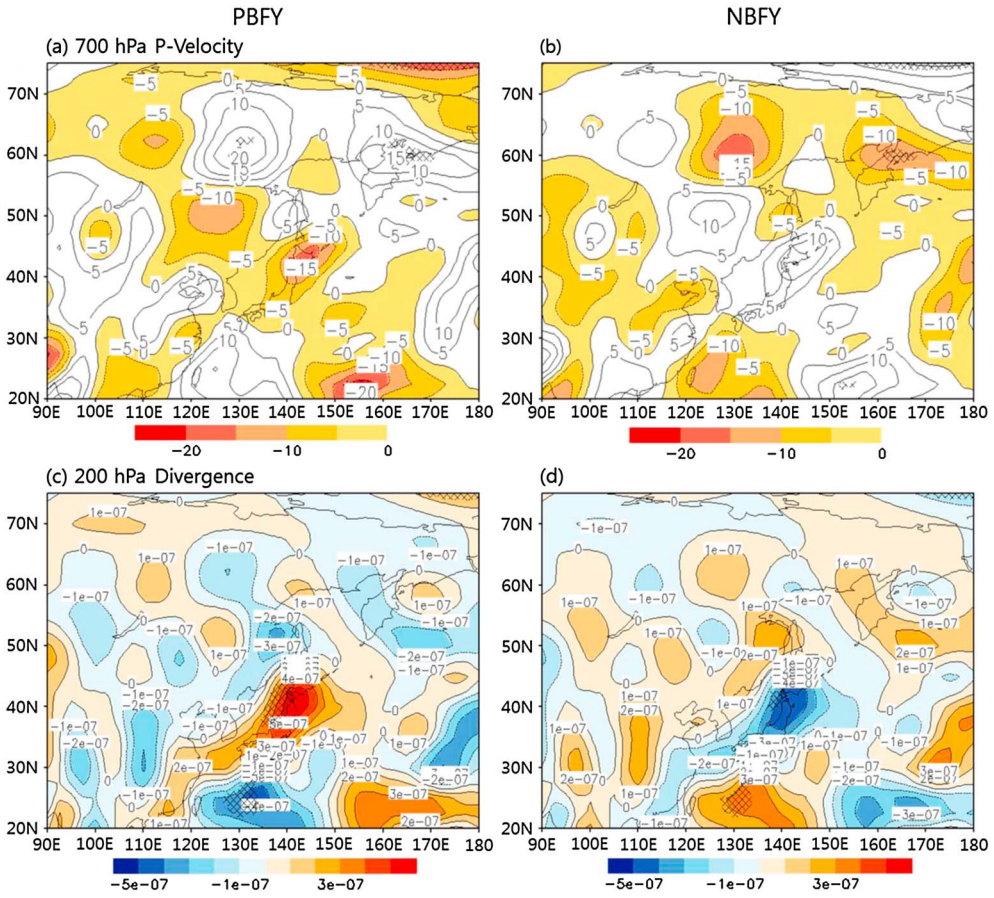

Figure 6. Composite anomalies of *P* velocity (hPa h^{-1}) and divergence (10^{-6} s^{-1}) during PBFY and NBFY over East Asia. The reticula indicate the regions of 10% significance level.

Figure 6 shows the 700 hPa vertical velocity and 200 hPa divergence. During PBFY, an updraft is dominant in 700 hpa over the Japan, Manchuria, and the East Sea (Figure 6a) in association with the convergence by cyclonic circulation at lower layer (Figure 5e) and the divergence in 200 hPa (Figure 6b). Such circulation pattern is likely to enhance the precipitation and the opposite scenario during NBFY.

The anomalous changes in precipitation and air temperature during PBFY and NBFY are shown in Figure 7. The precipitation increased around the Korean Peninsula and Japan and decreased around Taiwan (25°N) and the Sea of Okhotsk (60°N) including the North Pacific area associated with the atmospheric circulation shown in Figures 4, 5, and 6 during PBFY, and vice versa during NBFY. Summer temperature decreased over the wide region of increased precipitation, although the two regions did not coincide exactly. The correlation patterns in Figure 3 are the same as the composited anomalous features.

The vertical cross sections of composited potential temperature and *u*-*w* velocity anomaly fields along the latitudes averaged between 40 and 45°N during PBFY (Figure 8) illustrate that the cold air expands westward below 400 hPa level. In association with the cold air outbreak, surface air rises around 125–150°E throughout the whole vertical air column resulting in convergence and divergence of air at the surface and upper levels, respectively. The rising air that induces increased precipitation merges into upper level flows above the levels of 200–300 hPa, thereby strengthening the 200 hPa jet stream (Figure 5d). This clearly explains the cold air and increased precipitation over Korea and Japan centered around the East Sea during PBFY (Figures 7a and 7b).

4.4. Regional Influence of OK Blocking on Precipitation in Korea

As shown in Table 6 and Figure 3, OK BF is highly correlated with the summer temperature of the Korean Peninsula but not with precipitation. This unexpected result does not concur with the high correlation of the

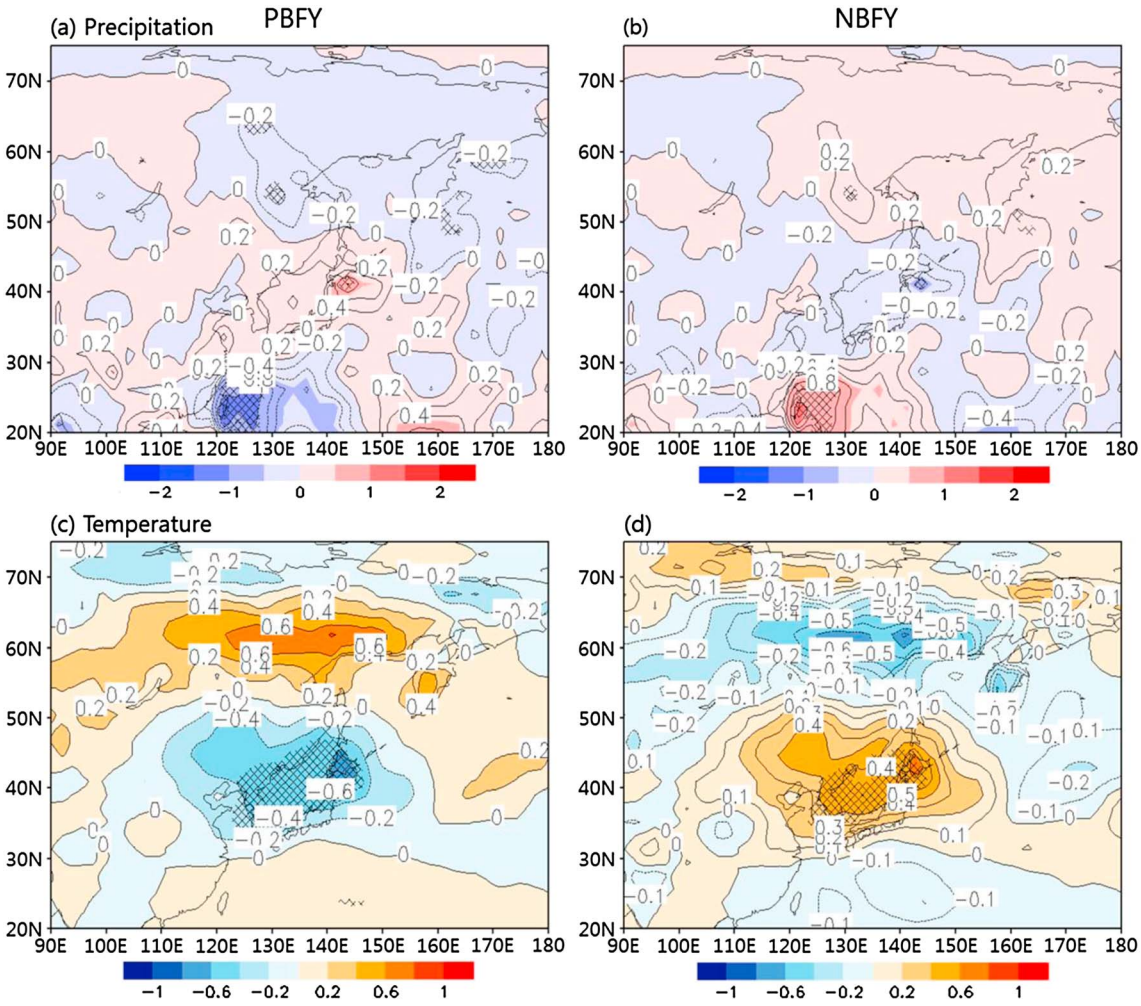

Figure 7. Same as in Figure 6 but for the precipitation (millimeters) and temperature (°C). The reticula indicate the regions of 10% significance level.

summer precipitation over the region with temperature [*Ahn et al.*, 1997]. Thus, in this study, using the in situ observation in South Korea, the composite distributions of summer temperature and precipitation for PBFY and NBFY were investigated (Figure 9). During PBFY (NBFY), the area-averaged temperature decreases (increases) by −0.41°C (0.36°C) throughout whole area. This result is consistent with the one shown in Figure 7. In particular, temperature changes in the eastern coast are larger than those in other areas due to the influences of the blocking over OK.

On the other hand, during PBFY, positive precipitation anomalies are shown in the central and eastern regions and negative anomalies appear simultaneously in some parts of the peninsula, particularly in the southwest region of South Korea. That is, the regional variations related to the blocking are revealed in the figure. The precipitation increases on the east coast where the influence of OK BF is large. The regional distribution of the precipitation seems to be influenced by the effect of Fohn-type winds. That is, due to the topographical location of the Taebaek Mountains extending in the meridional direction along the east coast of the peninsula, precipitation increases in the eastern regions when anomalous moist surface easterly wind blows from the East Sea (Figure 8), resulting in a decrease of precipitation on the leeward side of the mountain range. The fact that the increased/decreased precipitation does not correspond to the decreased/increased temperature during summer blocking indicates that the adiabatic cooling/warming effect associated with precipitation is not a one-to-one correspondence with temperature increase/decrease in a regional sense, although it still shows a negative correlation in a large-scale sense at the statistically insignificant level (Figure 3). Thus, the relatively low correlation between the summer blocking over OK and the precipitation of the Korean Peninsula (Table 6) is due to the regional precipitation deviations within the Korean Peninsula.

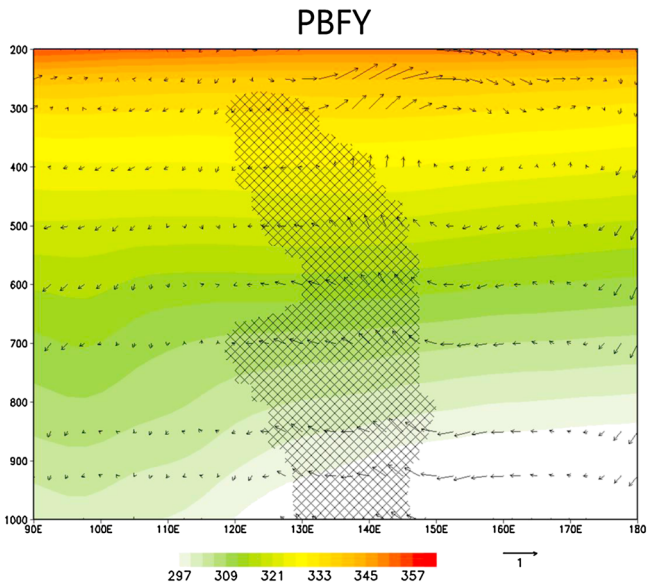

Figure 8. Vertical cross sections of composited potential temperature (°C) and *u*-*w* velocity (m/s) anomaly fields along the latitudes averaged between 40 and 45°N during PBFY. The reticula indicate the regions of the 10% significance level.

In addition, the distributions of temperature and precipitation changes over the peninsula during the PBFY and NBFY are quite similar and opposite in sign, which implies that the changes are quite systematic.

5. Summary and Conclusion

The East Asian monsoon system is one of the most energetic components of the global climate system [*Wang et al*., 2001], and the Northeast Asian summer monsoon known as *Meiyu*, *Changma*, and *Bai-u*, in particular, has great consequences over these regions in terms of agriculture, hydrology, and socioeconomics. As *Wang* [1992] insisted, the Northeast Asian summer monsoon is obviously affected by the blocking over OK.

In this study, blocking regions in summer were defined using the reanalysis data over the recent 30 years, and the changes in the atmospheric circulation over East Asia due to the influence of the blocking were investigated.

The summer blocking frequently occurred in NE (0°E–50°E), UR (50°E–80°E), OK (120°E–160°E), and NP (160°E–130°W). Particularly, NE BF and OK BF were most frequent at 5.21% and 5.81%, respectively, during summer. The PCA of 500 hPa geopotential heights revealed that the summer blocking was the first major mode in these regions.

Northeast Asia was mostly affected by OK blocking compared to the other blockings during the boreal summer. OK BF showed negative and positive correlations with summer temperature and precipitation, respectively, of Northeast Asia centered around the East Sea. The correlation coefficients between OK BF and temperature exhibited a tripole pattern with positive values at around 65°N and 25°N and a negative value at around 40°N. On the contrary, precipitation exhibited an opposite pattern of temperature in terms of correlation coefficients with OK BF. In particular, OK BF had a high correlation coefficient of −0.54 with summer temperature in the Korean Peninsula.

This indicates that the summer temperature and precipitation in this region were closely related to the OK blocking. According to the composite analysis for the years of PBFY, the OK High became strengthened and expanded, while the North Pacific High was weakened over the Korean Peninsula and Japan and an anomalously deep trough developed in the upper layer. As the cool OK High expanded over the region, the temperature decreased and the lower level air converged cyclonically, resulting in the increased precipitation, which induced the divergence in the upper layer and thereby strengthened the jet stream. On the contrary, during NBFY, the North Pacific High pressure was dominant and the geopotential field of upper layer became zonal over the East Asia. The jet was weakened in the upper layer, and anticyclonic circulation become

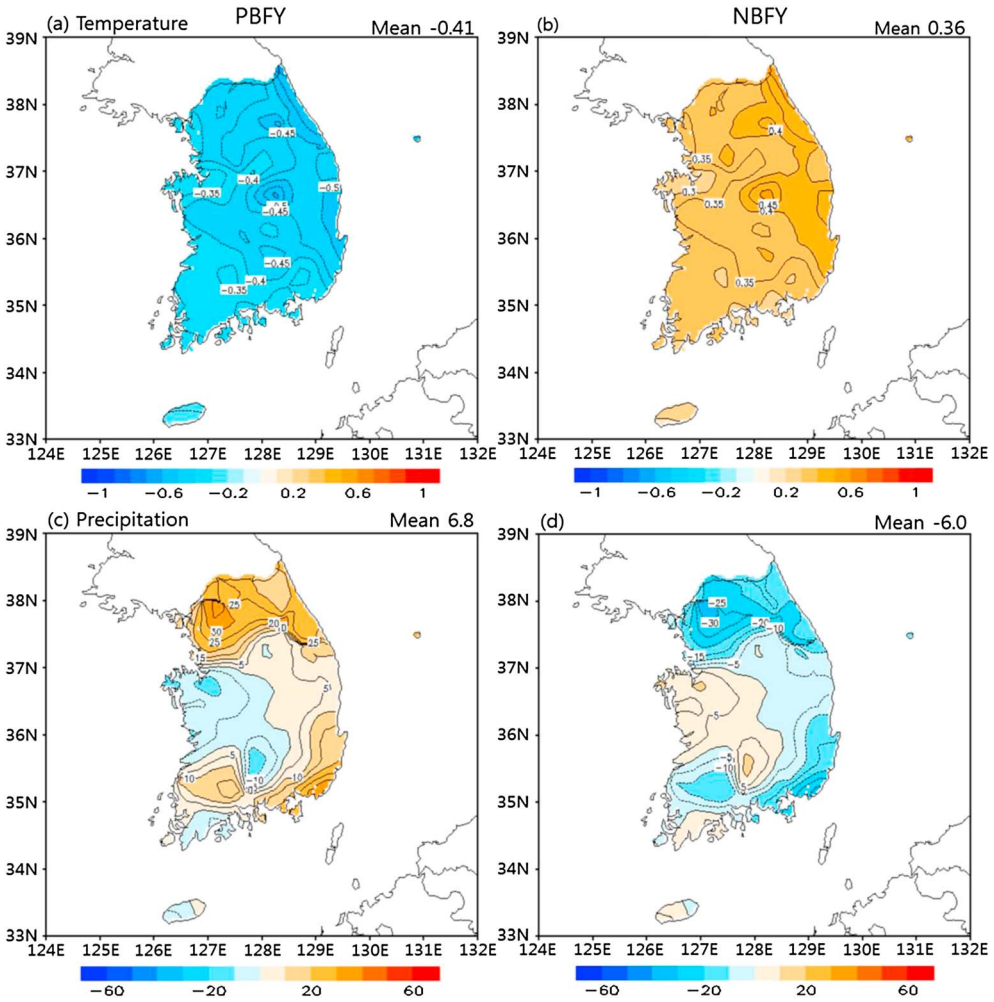

Figure 9. Distribution of temperature (°C) and precipitation (millimeter) in Korea in the case of PBFY field and NBFY field for JJA. The number in the figures' upper right corner is area-averaged values.

divergent in the lower layer, which induced the decreased precipitation over the East Sea/Sea of Japan. Due to the expansion of the warm North Pacific High, the temperature increased. Thus, the boreal summer OK blocking systematically influences the area as the most dominant mode.

In addition, NP, UR, and NE BFs increased but OK BF decreased in the positive AO years. During the El Niño years, blocking appeared more frequently in Europe, Sea of Okhotsk, and NP.

Acknowledgments

This work was carried out with the support of Rural Development Administration Cooperative Research Program for Agriculture Science and Technology Development under grant project PJ009353 and Korea Meteorological Administration Research and Development Program under grant CATER 2012–3100, Republic of Korea.

References

Ahn, J.-B., J.–H. Ryu, E.–H. Cho, and J.-Y. Park (1997), A study of correlations between air-temperature and precipitation of Korea and SST around Korean Peninsula, *J. Korean Meteorolog. Soc.*, *33*(2), 327–336, (abstract in English).

Barriopedro, D., R. Garcia-Herrera, A. R. Lupo, and E. Hernandez (2006), A climatology of Northern Hemisphere blocking, *J. Clim.*, *19*, 1042–1063.

Berggren, R., B. Bolin, and C. G. Rossby (1949), An aerological study of zonal motion, its perturbations and break-down, *Tellus*, *1*, 14–37.

Diao, Y., J. Li, and D. Luo (2006), A new blocking index and its application: Blocking action in the Northern Hemisphere, *J. Clim.*, *19*, 4819–4839.

Jang, Y.-K., and J.-G., Jhun (2004), Variation of western North Pacific convection and its influence on East-Asian summer monsoon, *J. Korean Earth Sci. Soc.*, *40*(3), 259–271, (abstract in English).

Kung, E. C., W. Min, J. Susskind, and C.-K. Park (1992), An analysis of simulated summer blocking episodes, *Q. J. R. Meteorol. Soc.*, *118*, 351–363.

Lee, H.-S., and J.-G. Jhun (2006), Two types of the Asian continental blocking and their relation to the East Asian monsoon during the boreal winter, *Geophys. Res. Lett.*, *33*, L22707, doi:10.1029/2006GL027948.

Lee, H.-S., and J.-G., Jhun (2007), Characteristics of atmospheric circulation over East Asia associated with unusual climate of Korea in winter 2006/2007, *J. Korean Earth Sci. Soc.*, *28*(3), 374–387, (abstract in English).

Lejenäs, H., and H. Øakland (1983), Characteristics of Northern Hemisphere blocking as determined from long time series of observational data, *Tellus*, *35A*, 350–362.
Lupo, A. R., and P. J. Smith (1995), Climatological features of blocking anticyclones in the Northern Hemisphere, *Tellus*, *47A*, 439–456.
Marques, R. F. C., and V. B. Rao (2000), Interannual variations of blocking in the Southern Hemisphere and their energetics, *J. Geophys. Res.*, *105*, 4625–4636, doi:10.1029/1999JD901066.
Matsueda, M. (2011), Predictability of Euro-Russian blocking in summer of 2010, *Geophys. Res. Lett.*, *38*, L06801, doi:10.1029/2010GL046557.
Pelly, J. L., and B. J. Hoskins (2003), A new perspective on blocking, *J. Atmos. Sci.*, *60*, 743–755.
Renwick, J. A. (1998), ENSO-related variability in the frequency of South Pacific blocking, *Mon. Weather Rev.*, *126*, 3117–3123.
Renwick, J. A., and J. M. Wallace (1996), Relationships between North Pacific wintertime blocking, El Nino, and the PNA pattern, *Mon. Weather Rev.*, *124*, 2071–2076.
Rex, D. F. (1950), Blocking action in the middle troposphere and its effect on regional climate, *Tellus*, *2*, 275–301.
Rimbu, N., and G. Lohmann (2011), Winter and summer blocking variability in the North Atlantic region—Evidence from long-term observational and proxy data from southwestern Greenland, *Clim. Past*, *7*, 543–555, doi:10.5194/cp-7-543-2011.
Shabbar, A., J. Hunag, and K. Higuchi (2001), The relationship between the wintertime North Atlantic oscillation and blocking episodes in the North Atlantic, *Int. J. Climatol.*, *21*, 355–369.
Tibaldi, S., and F. Molteni (1990), On the operational predictability of blocking, *Tellus*, *42A*, 343–365.
Trigo, R. M., I. F. Trigo, C. C. DaCamara, and T. J. Osborn (2004), Climate impacts of the European winter blocking episodes from the NCEP/NCAR reanalysis, *Clim. Dyn.*, *23*, 17–28.
Tyrlis, E., and B. J. Hoskins (2008), Aspects of a Northern Hemisphere atmospheric blocking climatology, *J. Atmos. Sci.*, *65*, 1638–1652.
Wang, Y. (1992), Effects of blocking anticyclones in Eurasia in the rainy season (Meiyu/Baiuseason), *J. Meteor. Soc. Japan*, *70*, 929–951.
Wang, Y., and A. R. Lupo (2009), An extra-tropical Air-Sea interaction over the North Pacific in association with a preceding El Niño episode in early summer, *Mon. Weather Rev.*, *137*, 3771–3785.
Wang, B., R. Wu, and K.-M. Lau (2001), Interannual variability of the Asian summer monsoon: Contrasts between the Indian and the western north pacific–east Asian monsoons, *J. Clim.*, *14*, 4073–4090.
Wiedenmann, J. M., A. R. Lupo, I. I. Mokhov, and E. A. Tikhonova (2002), The climatology of blocking anticyclones for the Northern and Southern Hemispheres: Block intensity as a diagnostic, *J. Clim.*, *15*, 3459–3473.
You, J.-E., and J.-B. Ahn (2012), The anomalous structures of atmospheric and oceanic variables associated with the frequency of North Pacific winter blocking, *J. Geophys. Res.*, *117*, D11108, doi:10.1029/2012JD017431.